Chin. J. Astron. Astrophys. Vol. 3 (2003), No. 4, 287–310
(http://www.chjaa.org or http://chjaa.bao.ac.cn)

Chinese Journal of Astronomy and Astrophysics

INVITED REVIEWS

Measuring the Fundamental Parameters of Hot Hydrogen-Rich White Dwarfs

M. A. Barstow *

Department of Physics and Astronomy, University of Leicester, University Road, Leicester, LE1 7RH, UK

Received 2003 June 2; accepted 2003 June 9

Abstract This review considers the observations of hot, hydrogen-rich white dwarf stars, with particular reference to measurements of temperature, surface gravity and composition. Spectroscopic data from a variety of wavelength ranges are required for this work and, in particular, the important contributions from optical, ultraviolet and extreme ultraviolet studies are discussed. Using the values of $T_{\rm eff}$ and log g determined for an individual white dwarf, estimates of mass and radius might be derived from the theoretical mass-radius relation. The issue of the accuracy of the theoretical mass-radius calculations and the prospects for making empirical tests using observational data are outlined.

Key words: stars: white dwarfs – ultraviolet – spectroscopy – mass – radius

1 INTRODUCTION

White dwarfs are among the oldest objects in the Galaxy. As remnants of all Galactic stars with initial masses below $\sim 8\,M_{\odot}$, they provide important laboratories for the study of evolutionary processes and the behavior of matter at extremes of temperature and density. Study of their space and luminosity distribution helps map out the history of star formation and can, in principle, determine the age of the galactic disk, so providing an important lower limit to the age of the Universe. Recently, it has been suggested that cool white dwarfs may account for a substantial fraction of the missing mass in the galactic halo (Oppenheimer et al. 2001). However, any of these results depend on our understanding of white dwarf evolution and, in particular, on predictions of the cooling rates. These in turn are affected by the mass, radius and photospheric composition of the stars.

Astronomers have known about the existence of white dwarf stars for 150 years, since the discovery of a companion to the brightest star in the sky, Sirius. Studying the regular wave-like proper motion of Sirius, F. W. Bessel revealed the presence of a hidden companion, with the pair eventually resolved by A. G. Clark in 1862 and the orbital period revealed to be 50 years. Later, a first spectroscopic study of the system by W. S. Adams revealed a great enigma. While

* E-mail: mab@star.le.ac.uk

the temperature of Sirius B was found to be higher than Sirius A, it was apparently 1000 times less luminous. This result could only be explained if Sirius B had a very small radius, $1/100\,R_\odot$ and similar to that of the Earth. However, with a known mass of $\sim 1\,M_\odot$ for Sirius B, the implied density of 1400 Tonnes m^{-3} was well above that of any form of matter known to 19th and early 20th century physicists. Within a number of years, a handful of stars similar to Sirius B were found, mostly in binaries. The term "white dwarf" was coined later, on the basis of the visual colour and small size, when compared to other stars.

The answer to the riddle of their structure stems from the development of the quantum statistical theory of the electron gas by Enrico Fermi and Paul Dirac. When atoms in a material are sufficiently close together, their most weakly bound electrons move freely about the volume and can be considered to behave like a gas. Almost all the electrons in the gas will occupy the lowest available energy levels. Any states with the same energy are said to be "degenerate". Hence, this gas is known as the "degenerate electron gas". Under conditions of extreme pressure the electrons are forced to occupy space much closer to the nuclei of the constituent atoms than in normal matter, breaking down the quantised structure of the energy levels. However, according to the Pauli exclusion principle, no two electrons can occupy the same quantum state, which has a finite volume in position-momentum space, so there is a limit where a repulsive force arising from this, the "electron degeneracy pressure", resists further compression of the material. Fowler (1926) showed that this pressure could support a stellar mass against gravitational collapse and proposed that this might explain the existence of white dwarfs. Combining this insight with the equations of stellar structure, Chandrasekhar (1931, 1935) determined the mass-radius relation for white dwarfs and the maximum mass ($1.4\,M_\odot$) that electron degeneracy pressure could support against gravity, the Chandrasekhar limit. This Nobel Prize winning work has been extended by subsequent developments, but the basic ideas remain unchanged.

Theoretical and observational study of stellar behaviour has provided white dwarfs with their evolutionary context as one end point of the process. In general terms, all stars with masses below about eight times that of the Sun will pass through one or more red giant phases before losing most of their original mass to form a planetary nebula. The remnant object, a white dwarf, is the core of the progenitor star. In the absence of any internal source of energy, the temperature of a white dwarf, after its birth, is determined by how rapidly stored heat is radiated into space. First estimates of white dwarf cooling times indicated that it would take several million years for the stars to fade to invisibility (Mestel 1952). Hence, white dwarfs are among the oldest objects in the galaxy. Since the galaxy is younger than the cooling timescales, the lowest temperature (oldest) white dwarfs yield a lower limit to its age.

The small radius and consequent low luminosity of white dwarfs has made them difficult to observe in detail. Hence, this original framework of their properties and astrophysical importance owed much more to theory than observation. Important physical characteristics such as temperature and surface gravity could, at first, only be based on broadband visual colours. During the past 25 years, there has been a revolution in astronomical observation techniques. The advent of electronic detectors and improvements in sensitivity of ground-based telescopes has been matched by the opening of ultraviolet, extreme ultraviolet and X-ray wave bands by satellite-borne observatories. A direct result of this has been a remarkable transformation in our observational knowledge concerning white dwarfs and major advances in our understanding of their physical characteristics and evolution. This review concentrates on some of the most important recent work contributing to studies of the white dwarf mass-radius relation and white dwarf composition from ultraviolet observations, concentrating on the most numerous group, which have hydrogen-rich atmospheric compositions. Particular reference will be paid to measurements of temperature, surface gravity and composition, using spectroscopic data from a variety of wavelength ranges. The importance of $T_{\rm eff}$ and log g, determined for an individual white dwarf, in estimating of mass and radius will be described, and the dependence of such determinations on theoretical calculations of the mass-radius relation discussed.

2 CLASSIFICATION OF WHITE DWARFS

The basis for understanding the nature of most stars is analysis of their optical spectra and classification according to the characteristics revealed. A number of physical processes can alter the atmospheric composition of a white dwarf as it cools. As noted by Schatzmann (1958), the strong gravitational field ($\log g \sim 8$ at the surface) causes rapid downward diffusion of elements heavier than the principal H or He component. Hence, Schatzmann predicted that white dwarf atmospheres should be extremely pure. Consequently, the spectra should be devoid of most elements, showing signatures of only hydrogen and, possibly, helium. White dwarfs are thus divided into two main groups according to whether or not their spectra are dominated by one or other of these elements. The hydrogen-rich stars are given the classification DA, while the helium-rich white dwarfs are designated DO if HeII features are present (hotter than about 45 000 K) and DB if only HeI lines are visible. Small numbers of hybrid stars exist, with both hydrogen and helium present. In these cases, two classification letters are used, with the first indicating the dominant species. For example, DAO white dwarfs are mostly hydrogen but exhibit weak HeII features.

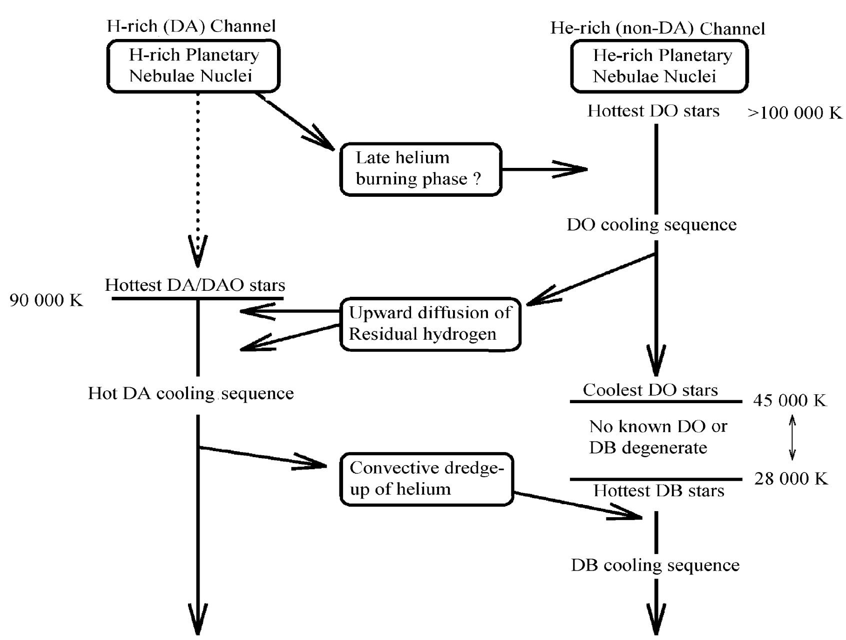

Fig. 1 Schematic description of the production of H-rich and He-rich branches of white dwarf evolution.

The above classification scheme applies only to white dwarfs with temperatures above $\sim$10 000 K, when the H and He energy levels are sufficiently populated above the ground state to produce detectable features. However, at lower temperatures, although H and/or He may be present these elements are no longer directly detectable. Cool white dwarfs are divided into three main groups. DC white dwarfs have continuous, completely featureless spectra; DZ white dwarfs are He-rich and have only metal lines visible; DQ white dwarfs show carbon features. Figure 1 summarises the current thoughts regarding the relationships between the hot white dwarf groups along with the principal mechanisms that provide evolutionary routes between them.

However, the gravitational force can be countered by that of radiation pressure which acts outward to support heavy elements in the atmosphere, a process termed "radiative levitation". Another mechanism that can mix elements that have settled out in the stellar atmosphere is convection. If the convective zone reaches down to the base of the atmosphere then heavy elements can be dredged back up into the outer atmosphere. A further complication is that material can also be accreted from the interstellar medium (ISM).

The emergence from the Asymptotic Giant Branch (AGB) of two main white dwarfs channels, whose compositions are dominated by H or He, is beginning to be understood in relation to mass-loss processes and the number of times a star ascends the giant branch. However, a demonstrable temperature gap in the He-rich cooling sequence, between the DO and DB groups, cannot yet be explained.

3 SPECTROSCOPIC MEASUREMENTS OF EFFECTIVE TEMPERATURE AND SURFACE GRAVITY

3.1 Balmer Line Studies

To solve the problems of white dwarf evolution it is necessary to measure a number of basic parameters for a significant fraction of the white dwarf population. To set a star in its evolutionary context we need to know its effective temperature and surface gravity. In early studies, these were estimated from broadband photometric observations, coupled with simple assumptions about the relation between temperature and spectral shape (e.g. the assumption of a blackbody). In modern astronomy we now have access to high signal-to-noise spectra and sophisticated stellar atmosphere models and associated synthetic spectra for comparison with the data.

For the largest group of white dwarfs, the DA stars, there is a very powerful analysis technique based on the hydrogen Balmer absorption lines. The strength and shape of an individual line depends on the temperature and density structure of the atmosphere in which it is formed, which in turn are determined by the temperature and gravity of the star. Specifically, line strengths depend on the populations of atoms at the energy levels involved in a particular transition, which are temperature sensitive. An "indefiniteness" in the energy levels for individual atoms leads to line broadening. This arises from two sources. First, perturbations of the radiative wave train through collisions with other particles in the gas causes *pressure broadening*, which depends mainly on gravity. Secondly, temperature dependent gas motions lead to *Doppler broadening* of the lines. Figure 2 shows a selection of optical spectra of hot DA white dwarfs ordered by decreasing temperature. By comparing the observed line profiles with predicted ones simultaneously for at least four lines it is possible to obtain a unique solution for $T_{\rm eff}$ and log g for any DA white dwarf. This procedure, illustrated in Fig. 3 for the hot DA white dwarf PG1342+444, allowed the first systematic spectroscopic study of a large sample of stars (Bergeron et al. 1992). An important feature of this analysis technique is that it is completely objective. Rather than making a purely visual comparison and selection of the best-fit synthetic spectrum, the best match is determined by a goodness of fit statistic such as the χ^2 test. In addition, this allows formal determination of the statistical errors by examining the variation of χ^2 with $T_{\rm eff}$ and $\log g$.

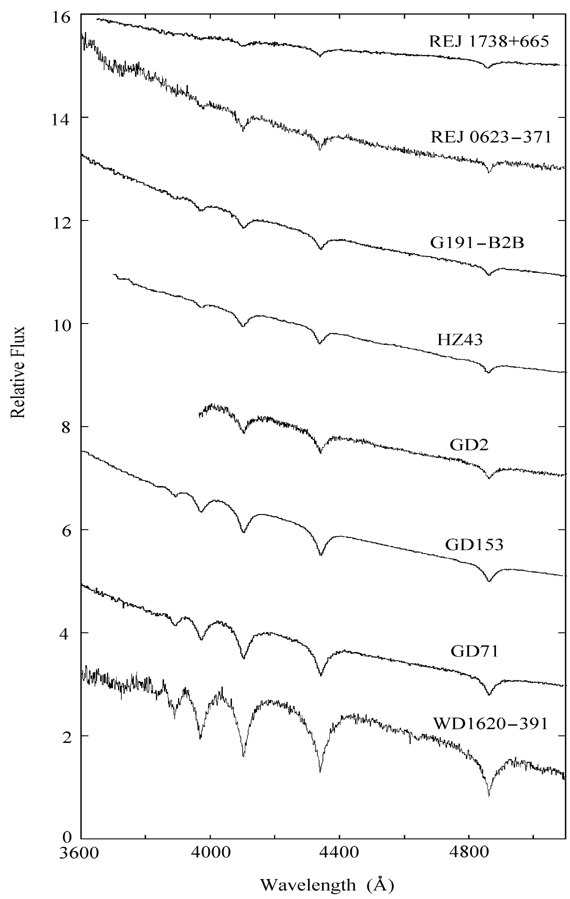

Fig. 2 Sample of Balmer line spectra for a selection of hot DA white dwarfs in order of decreasing temperature from the top of the figure.

The study of Bergeron et al. (1992) was based on the use of pure H model atmospheres computed under the assumption of Local Thermodynamic Equilibrium (LTE), that the ion and level populations are entirely specified by the Saha and Boltzmann equations. Further work has involved the use of better non-LTE models, where the ion and level populations are determined by statistical equilibrium calculations, which take into account the radiation field besides the collisional interactions between particles. In addition, the assumed composition has an influence on the calculated Balmer line profiles. Barstow et al. (1998) assessed how this affects the temperature and gravity determinations, noting that the inclusion of significant quantities of metals lowers the inferred temperature, particularly for the hottest objects.

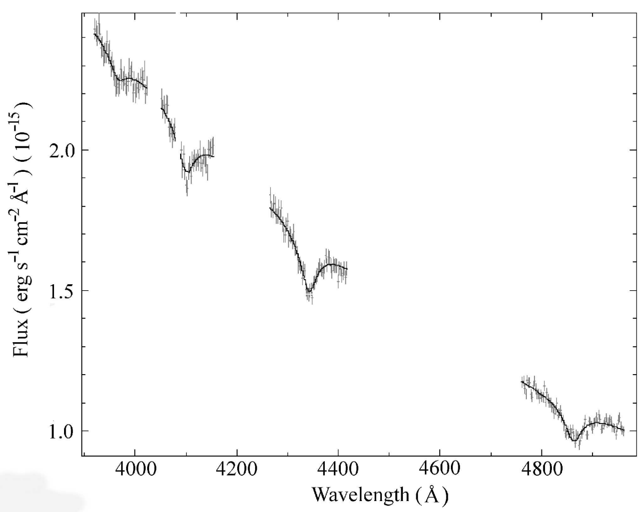

Fig. 3 Example of the technique of comparing the Balmer lines from the spectrum (error bars) of the hot DA white dwarf PG1342+444, with the synthetic line profiles from stellar atmosphere calculations (solid curve).

3.2 Lyman Line Studies

In the samples studied using the Balmer line technique, the majority of the stars are isolated objects. If any are in binaries, they are either wide, resolved systems or the companions are late-type dwarfs, where the white dwarf can be spectroscopically isolated. However, when a white dwarf binary companion is spatially unresolved and of type K or earlier, the white dwarf visible signature is hidden in the glare of the more luminous object (e.g. Fig. 4) and, therefore, the Balmer lines cannot be used for determination of $T_{\rm eff}$ or $\log g$. If the companion is not earlier than type A, the white dwarf spectrum dominates in the far-UV (see Fig. 4) and the Lyman lines are accessible, allowing them to be used for determination of $T_{\rm eff}$ and $\log g$. A well-known illustration of this is the DA+K star binary V471 Tauri, which has been extensively studied and where the Lyman series spectrum obtained by the *ORFEUS* mission was used to obtain the first accurate measurements of $T_{\rm eff}$ and $\log g$ (Barstow et al. 1997).

While the Lyman α line is encompassed by the spectral coverage of *IUE* and *HST* data, a single line cannot provide an unambiguous measurement of $T_{\rm eff}$ and $\log g$. Access to the full Lyman series lines has been provided by the short duration missions of the Hopkins Ultraviolet Telescope (*HUT*) and Orbiting and Retrievable Far and Extreme Ultraviolet Spectrometers (*ORFEUS*). They provided observations of a number of white dwarfs at wavelengths down to the Lyman limit, yielding a first opportunity to compare Balmer and Lyman line measurements systematically. Barstow et al. (2001) carried out an evaluation of all the available archival data for these missions, including some early spectra from the Far Ultraviolet Spectroscopic Explorer (*FUSE*). Comparing the results with those from the standard Balmer line analysis, they found general overall good agreement between the two methods. However, significant differences were noted for a number of stars. These differences were not always consistent in that sometimes the Balmer temperature exceeded that derived from the Lyman lines and in other instances was lower, which would not be expected if the problems arose from the limitations of the stellar atmosphere calculations and the treatment of the Lyman and Balmer line broadening. The most likely conclusion was that systematic effects arising from the observations, the data reduction and the analysis were responsible for the discrepancies.

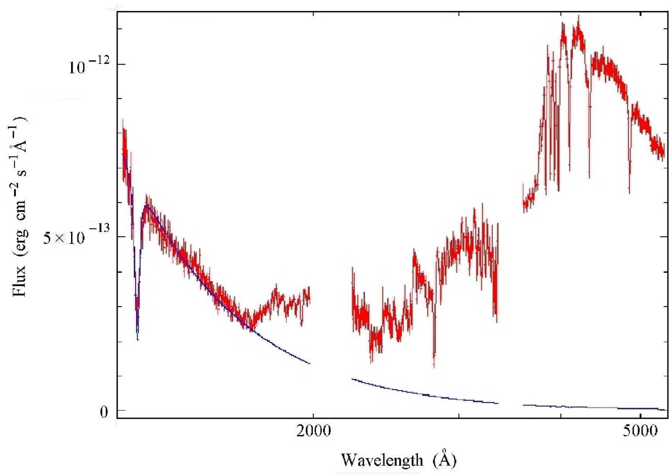

Fig. 4 UV and optical spectrum of the DA white dwarf plus A8-F2 main sequence star binary system BD+27°1888 (error bars). A synthetic DA white dwarf model spectrum is shown for comparison (smooth curve).

More recently it has been possible to re-examine the issue of the Lyman line analysis with a greatly expanded far-UV data set available from the *FUSE* mission. These spectra cover the complete Lyman line series from β to the series limit, excluding Lyman α, and cover a larger number of stars, particularly at values of $T_{\rm eff}$ above 50 000 K (a range that was sparsely sampled by Barstow et al. 2001b). In addition, *FUSE* has observed some of the targets many times, for purposes of monitoring the instrument calibration, which provides a powerful tool for examining systematic effects in the instrument and analysis procedure. Figure 5 shows a sample of typical *FUSE* spectra, ordered by decreasing temperature from $T_{\rm eff}$ ~70,000 K down to $T_{\rm eff}$ ~20,000 K, and Fig. 6 the results of the Lyman line analysis for GD659.

With the availability of the *FUSE* data archive and observations from Guest Observer programmes, Barstow et al. (2003a) examined the use of the Lyman series to determine the values of $T_{\rm eff}$ and $\log g$ for a sample of 16 hot white dwarfs. Having a source of data produced by a single instrument and processed with a uniform pipeline, made it possible to eliminate some of the possible systematic differences between observations of the same or different stars associated with different instruments. However, it is clear from this study that systematic errors in the overall observation, data reduction and analysis procedures dominate the measured uncertainties. Using the scatter in values derived from multiple observations of some stars it was possible to determine more realistic errors in the measurements than obtained just from the statistical error values. The new results partially reproduce the earlier study, where a more limited stellar sample was studied, showing that Balmer and Lyman line determined temperatures are in good agreement up to ~50 000 K. However, above this value there is an increasing systematic difference between the Lyman and Balmer line result, the former yielding the higher temperature (Fig. 7). At the moment, there is no clear explanation of this effect but it is most likely associated with deficiencies in the detailed physics incorporated into the stellar model atmosphere calculations. Even so, the data do demonstrate that, for temperatures below 50 000 K, the Lyman lines give reliable results. Furthermore, for the hotter stars, a useful empirical calibration of the relationship between the Lyman and Balmer measurements has been obtained, that can be applied to other *FUSE* observations.

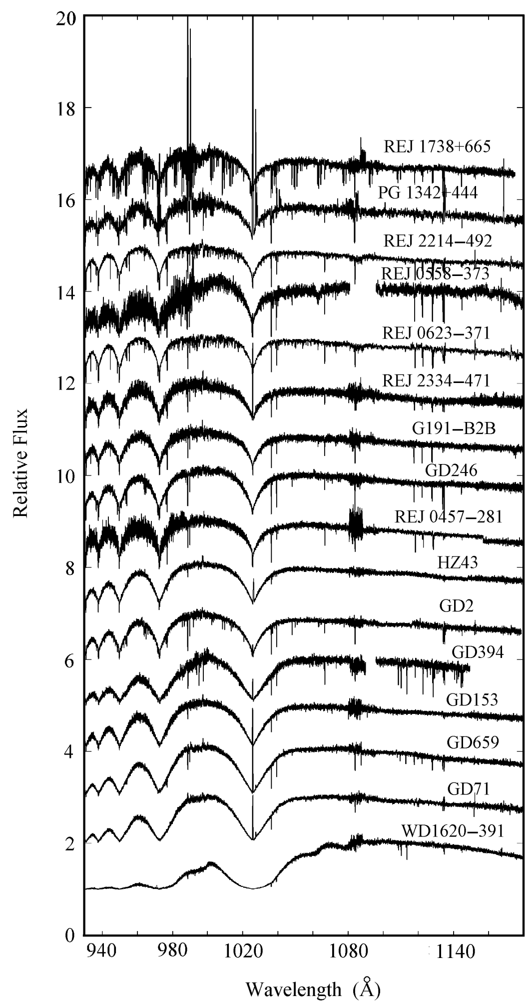

Fig. 5 Sample *FUSE* spectra for all the DA white dwarfs in order of decreasing $T_{\rm eff}$ (as measured with the Balmer lines) from the top of the figure.

4 WHITE DWARF MASSES AND RADII

Two of the most important physical parameters that can be measured for any star are the mass and radius. They determine the surface gravity by the relation $g = GM/R^2$. Hence, if $\log g$ is measured the mass can be calculated provided the stellar radius is known. One outcome of Chandrasekhar's original work on the structure of white dwarfs was the relationship between mass and radius, arising from the physical properties of degenerate matter. Further theoretical work yielded the Hamada-Salpeter zero-temperature mass-radius relation (Hamada & Salpeter 1961). However, as has already been seen in this review, white dwarfs do not have zero temperature, indeed many are very hot. Hence, the Hamada-Salpeter relation is only a limiting case and the effects of finite temperature need to be taken into account. Evolutionary calculations, where the radius of a white dwarf of given mass decreases as the star cools, have been carried out by Wood (1992, 1995), Blöcker (1995) Blöcker et al. (1997) and others. The most recent Blöcker models are full evolutionary calculations from the AGB, while those of Wood have a semi-arbitrary starting point for the hottest models.

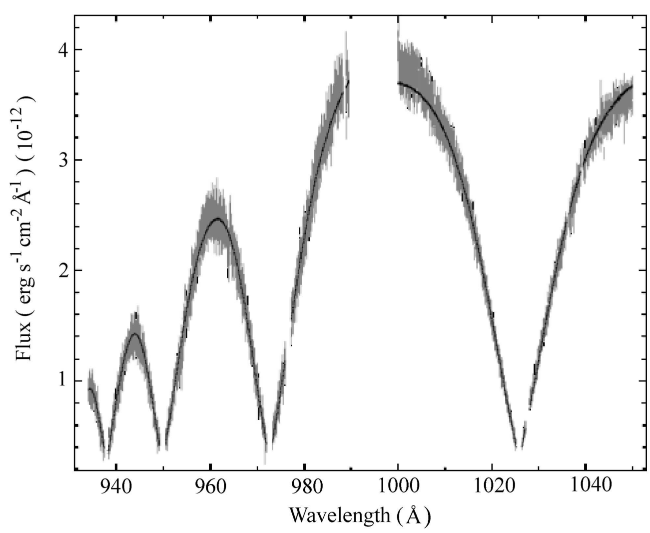

Fig. 6 Lyman $\beta - \varepsilon$ lines from a *FUSE* spectrum of the hot DA white dwarf GD659 (grey error bars), showing the comparison with the best-fit synthetic model spectrum (black curve). Data gaps arise from removal of the Lyman geocoronal emission and interstellar absorption. Other strong interstellar lines have also been removed for the analysis.

Even the earliest measurements of surface gravity gave a strong hint that the distribution of $\log g$ values and, therefore, of mass was very narrow. This supposition was subsequently confirmed by the work of Bergeron et al. (1992) and other authors. The most recent study of Napiwotzki et al. (1999), based on a EUV-selected sample of white dwarfs, yields a peak mass of $0.59\,\mathrm{M}_\odot$ and an estimated FWHM of $\sim 0.15\,M_\odot$ for the distribution. It is interesting that the EUV-selected sample yields a larger fraction of high-mass white dwarfs than the studies based entirely on optical surveys. This preferential detection of high mass objects in the hot DA sample probably arises from a drop in neutrino cooling which leads to a slowing down of the evolution of the highest mass white dwarfs.

The narrowness of the observed mass distribution is a direct consequence of the evolution of single stars, with masses from $1\,M_\odot$ up to $\sim 8\,M_\odot$. While the details of the relationship between the initial mass of the progenitor star and the final white dwarf mass are not particularly well understood, it is clear that the small dispersion in the white dwarf masses is related to a similarly small range of stellar core masses and the fact that most of the outer stellar envelope is expelled through several phases of mass loss along the AGB. Importantly, any white dwarf with masses outside the approximate range $0.4 - 1.0\,M_{\odot}$ cannot arise from single star evolution and must have an origin in a binary, where mass exchange has taken place.

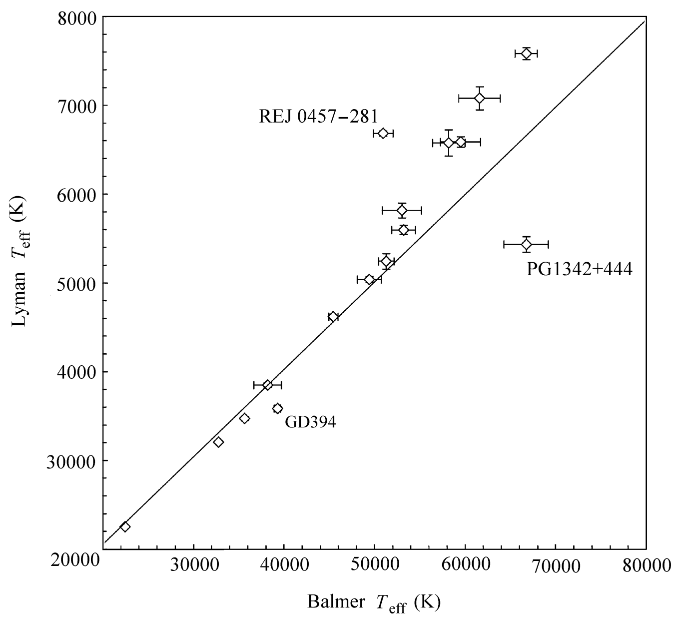

Fig. 7 Scatter plot of the simple mean values of $T_{\rm eff}$ measured using the ground-based Balmer and FUSE Lyman lines. The error bars are calculated from the variance of the values in multiple observations or are the statistical 1σ error for single observations. The solid line corresponds to equal Balmer and Lyman line temperatures.

While, the basic model of the white dwarf mass-radius relation, which is used to derive masses from the spectroscopic data, is not in serious doubt, it is interesting to note that opportunities for direct observational tests of the work are rare. This is particularly true of the higher-level refinements that take into account the finite stellar temperature and details of the core/envelope structure, discussed above. Varying the assumed input parameters in these models can lead to quite subtle, but important differences in the model predictions. To test these requires independent measurements of white dwarf mass that can be compared with the spectroscopic results. Such information can be obtained dynamically, if the white dwarf is part of a binary system, or from the gravitational redshift ($V_{\rm gr}[{\rm km\ s^{-1}}] = 0.636\,M/R$), for which an accurate systemic radial velocity is required (often only possible in a binary). An additional important constraint is knowledge of the stellar distance. We have such data for only a very few white dwarfs. The four best examples (i.e. where we have the most complete and accurate information) are 40 Eri B, Procyon B, V471 Tauri B and Sirius B, where we can combine the assembled data with the *Hipparcos* parallax to test the mass radius relation (Fig. 8). While there is good agreement between the observation and theory, there nevertheless remains a high degree of uncertainty in the mass determinations. As a result, for example, it is not possible to distinguish between different models, such as those with "thin" or "thick" H envelopes.

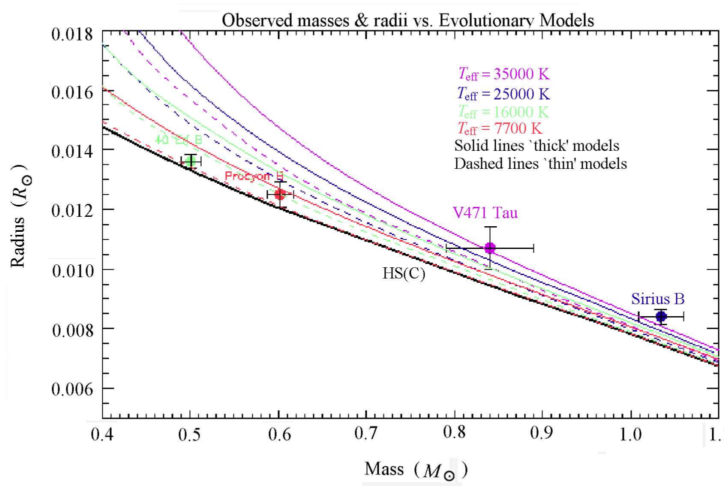

Fig. 8 Comparison of mass estimates for 40 Eri B, Procyon B, V471 Tau B and Sirius B with the evolutionary models of Wood (1995), displayed at various temperatures and with "thin" and "thick" H envelopes. The solid limiting curve represents the Hamada-Salpeter zero temperature relation for a carbon core (figure produced by Jay Holberg).

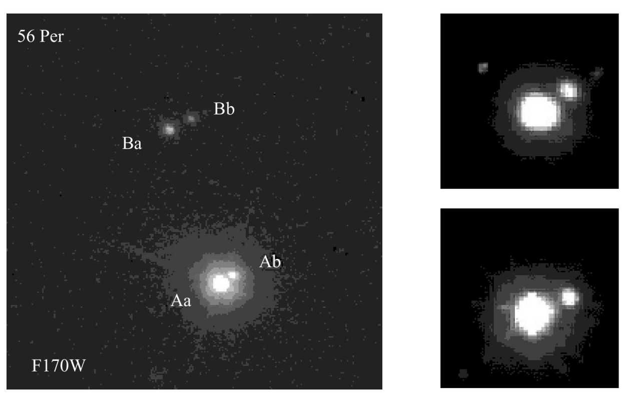

Fig. 9 Wide Field Planetary Camera image of the binary 56 Per, where each component (A & B) is itself resolved into a pair (right). Successive images of the Aa/Ab pair taken $\sim$ 18 months apart clearly show the orbital motion of the system.

Clearly it would be very desirable to extend the sample of white dwarfs for which we have dynamical masses, gravitational redshifts and accurate parallaxes to more objects and, possibly, explore a wider range of masses and temperatures. A major result of the EUV sky surveys conducted by *ROSAT* and *EUVE* was the discovery of many unresolved binary systems containing white dwarfs and companion spectral types ranging from A to K (e.g. Barstow et al. 1994; Burleigh, Barstow & Fleming 1997; Vennes, Christian & Thorstensen 1998). Therefore, a large pool of potential sources exists, for which the required information may be forthcoming in the future. In most of these cases Lyman series observations will be essential to determine $T_{\rm eff}$ and $\log g$. Importantly, although most isolated white dwarfs were too faint for *Hipparcos* parallax measurements, the presence of the bright binary companion means that *Hipparcos* data is often available. Although these systems are not resolved in ground-base observations, the HST Wide Field Planetary Camera 2 has observed most of them in the UV, to measure their separations, or at least provide improved constraints. Images of 18 binary systems resolve 9 objects (Barstow et al. 2001a). Figure 9 shows one of the most interesting examples, 56 Per, a known binary in which each component has been resolved into a pair, making it a quadruple star system. The white dwarf is a companion to 56 Per A and is labeled 56 Per Ab in the image. At a distance of 42 pc, the measured 0.39 arcsec separation indicates a binary period of ~ 50 years for the Aa/Ab system. Therefore, the orbital motion of the two stars should be readily apparent with repeated exposures on timescales $\sim 1 - 2$ years, from which a dynamical white dwarf mass can ultimately be obtained. This is clearly demonstrated in Fig. 9 which shows a zoomed view of the Aa/Ab pair from the main image and, on a similar scale, a second image obtained ~ 18 months after the first.

5 ELEMENT ABUNDANCES FROM EUV AND UV SPECTROSCOPY

5.1 The Historical Picture

Determination of the photospheric He and heavy element content provides important information on the prior evolutionary history of a white dwarf and the physical effects of mechanisms that may compete to alter the observed composition of the atmosphere. While H and He are readily detected in the visible region of the spectrum, it is much harder to detect other elements, unless the abundances are very high. For example, absorption lines from CIV can be seen in many He-rich white dwarf spectra, with an abundance (C/He) of $\sim 10^{-2}$. However, in the DA stars, the C/H ratio is usually much lower and the carbon undetectable in the visible band. Indeed, He is also hard to detect, requiring abundances in excess of a few times 10^{-3} in the visible band. Therefore, the most important and useful transitions, in particular for many resonance lines of elements heavier than H and He lie in the far-ultraviolet (far-UV, 1000–2000Å), extreme ultraviolet (EUV, 100–1000Å) and soft X-ray (about 10–100Å) regions of the spectrum. Hence, access to these wavebands has been crucial for understanding the detailed atmospheric composition of white dwarfs. Unfortunately, absorption of the incident radiation by the Earth's atmosphere prevents ground-based observations and the development of space observatories has largely determined what could be achieved.

The first far-UV and X-ray observatories, flown in the early 1970s, were largely insensitive to white dwarfs. Nevertheless, a handful of stars were detected stimulating future work. Subsequently, key contributions have been made by a succession of missions beginning with the International Ultraviolet Explorer (*IUE*), and continuing with Roentgen Satellit (*ROSAT*), the Extreme Ultraviolet Explorer (*EUVE*) and Hubble Space Telescope (*HST*).

Since the hottest white dwarfs radiate the majority of their energy in the soft X-ray and EUV regions of the spectrum, they are likely to provide a significant fraction of the ionising photons in the local interstellar medium (LISM). Hence, one original motivation for observing white dwarfs in the far-UV was to study their circumstellar environments and the LISM, by observing absorption lines projected onto their otherwise smooth hot blue continua. Such features were detected and usually associated with low ionisation stages of elements, usually of CI, CII, NI, NII, OI, OII, SiI, SiII and SiIII, although sulphur has also been seen. Since these interstellar lines are weak and narrow, they are only visible at high resolution ($R > 20\,000$). An example is a small section of the high-resolution spectrum of the DA white dwarf REJ0558–373, recorded with the Space Telescope Imaging Spectrograph (STIS) onboard *HST* (Fig. 10), which shows the interstellar 1260.4Å line of SiII together with photospheric NV.

Interstellar absorption features typically arise from low ionisation species. However, high ionisation transitions were detected in some of the first *IUE* echelle spectra of white dwarfs (e.g. Bruhweiler & Kondo 1983). Initially, it was suggested that these features were associated with circumstellar material, excited by the strong UV and EUV flux of the white dwarf (Dupree & Raymond, 1982). However, determination of the photospheric velocities of several stars, coupled with the *EXOSAT* EUV spectrum of Feige 24 (Vennes et al. 1988), established that the observed features were photospheric in origin. Nevertheless, it was far from clear whether stars like Feige 24 or the similar G191-B2B were typical of the DA population or if stars with pure H atmospheres were more representative.

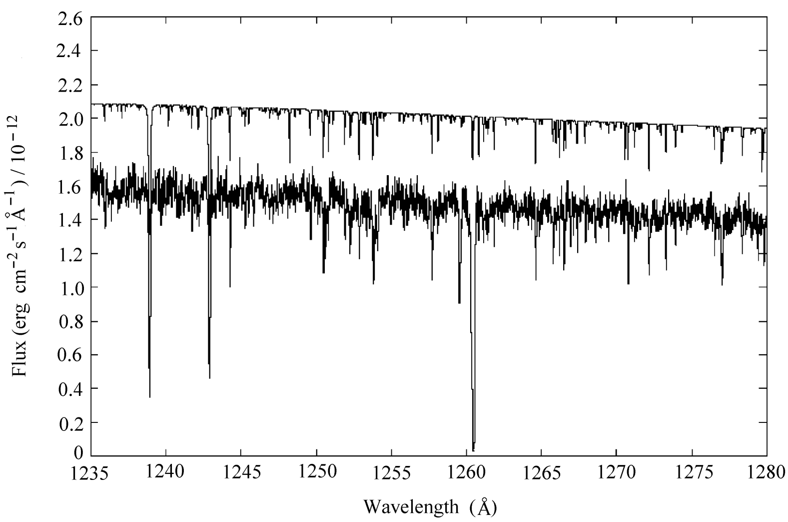

Fig. 10 1230Å to 1280Å region of the STIS spectrum of REJ0558–373, showing photospheric absorption lines of NV (1238.821/1242.804Å) and large numbers of Ni lines. The best-fit synthetic spectrum is shown offset for clarity. The strong line near 1260Å, present in the observation but not in the model, is interstellar SiII.

Ultimately, the larger statistical sample of the *ROSAT* WFC EUV sky survey provided the solution to that question. The emergent EUV continuum radiation from a white dwarf is very sensitive to the presence of absorbing heavy elements, which suppress the flux compared to the level that would be expected from a pure H atmosphere. In a sample of $\sim$ 100 stars studied by *ROSAT,* it is clear that the EUV and soft X-ray luminosities of objects hotter than about 50 000 K are much lower than expected, while white dwarfs below this temperature typically have luminosities consistent with pure H envelopes (Barstow et al. 1993; Marsh et al. 1997). In most of the hottest white dwarfs, broadband soft X-ray and EUV photometry was able to rule out helium as the sole source of opacity, indicating that heavier elements play a significant role. This result is consistent with the view that radiation pressure can counteract the downward diffusion of heavy elements induced by gravity in the hottest white dwarfs (e.g. Chayer et al. 1995).

5.2 UV Spectroscopy

Broadband fluxes do not provide sufficient information to determine either the specific absorbing species or to estimate their abundances. Hence, the survey data must be complemented by more detailed spectroscopic observations in the EUV and far-UV, but, because of limits on the available observing time, for a smaller number of objects. Prior to the shutdown of the *IUE* satellite, high-resolution ($R \sim 20\,000$) echelle spectra were routinely obtained. These were very important for the initial exploitation of interesting white dwarfs newly discovered by the ROSAT survey (e.g. Holberg et al. 1993, 1994). However, the *IUE* spectra had a typical limiting signal-to-noise of $\sim 3:1$ and a limiting magnitude $\sim V = 15$ for practical exposure times. Subsequently, an effective technique was developed for coadding multiple exposures to improve signal to noise. This has been further enhanced, by reprocessing the original data, yielding a valuable archive of high dispersion white dwarf spectra (see Holberg et al. 1998). The overall quality of the archive is quite variable depending on the number of exposures taken of each star. Typically, those stars suspected of containing heavy elements have been observed more often, achieving a higher ultimate signal to noise than single observations of apparently pure H white dwarfs. An example of the result of combining several exposures is seen in Fig. 11, which shows a region of the coadded *IUE* spectrum of G191–B2B (14 exposures). This is compared with a single optimally exposed spectrum of PG1234+482, showing a clear difference in signal-to-noise.

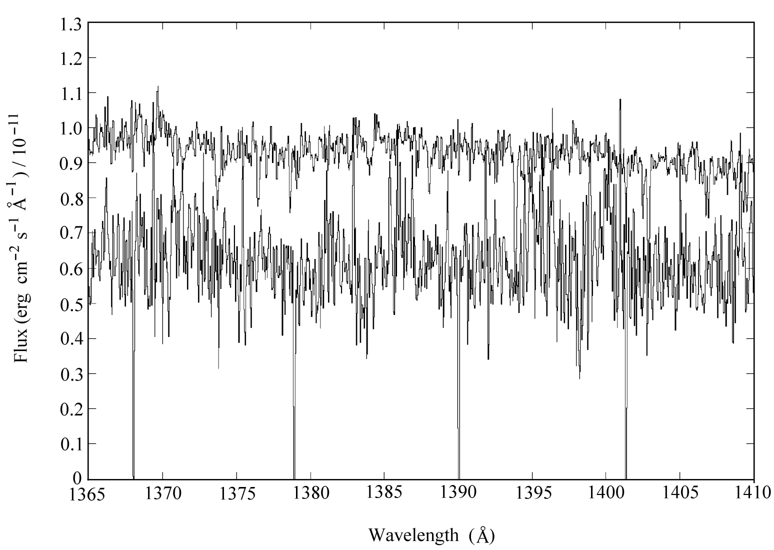

Fig. 11 Comparison of the signal-to-noise achieved from a co-added *IUE* spectrum (top, of G191–B2B) with a single exposure (bottom, of PG1234+482). The lower spectrum has been scaled to the flux of the upper one and then offset for clarity.

In parallel with the latter years of the operation of *IUE*, the Hubble Space Telescope has given further access to the far-UV waveband. However, with a considerably larger aperture than *IUE*, it is possible to observe fainter targets and achieve greater signal to noise. Initially, high dispersion ($R \sim 40\,000 - -100\,000$) spectra were obtained by the Goddard High Resolution Spectrograph (GHRS) but, unlike the *IUE* echelle data could only cover a narrow (30–40Å) waveband in a single exposure. Hence, complete wavelength coverage similar to that obtained by *IUE* would have required a large number of individual exposures, yielding prohibitively long observations. The replacement of the GHRS by the Space Telescope Imaging Spectrograph (STIS) in 1997 provided an instrument with improved throughput and *IUE*-like wavelength coverage while retaining the high-resolution spectroscopic capabilities. In the E140M (medium echelle) mode, the resolving power is $R \sim 40\,000$ and far-UV coverage from $\sim 1150 - 1750$Å. The highest resolution E140H grating only gives a span of ~ 200Å at a time but can be tilted to build up full wavelength coverage in successive exposures. The capabilities of STIS are illustrated in the E140H exposure of G191–B2B in the region of the CIV resonance doublet, the equivalent *IUE* observation is also shown for comparison (Fig. 12). It is interesting to see how the apparent single components seen by *IUE* have a clear asymmetric appearance indicating that each is a pair of blended lines, in this case circumstellar and photospheric contributions.

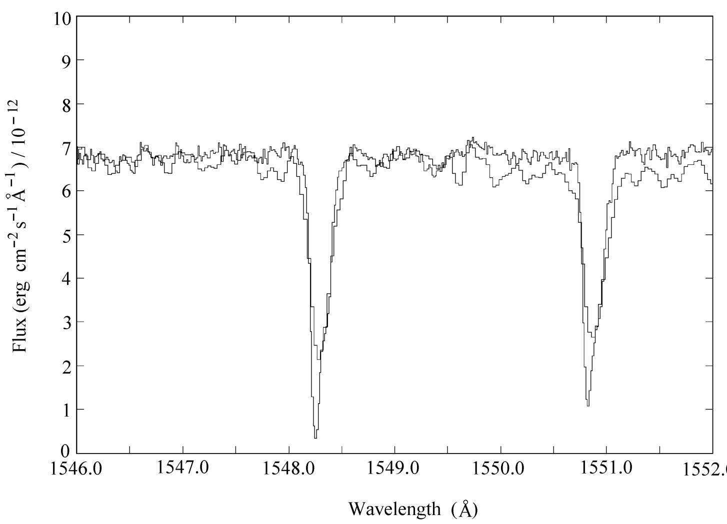

Fig. 12 Comparison of the coadded *IUE* spectrum of G191–B2B with that obtained at higher spectral resolution by the STIS instrument on HST, in the region of the CIV 1548/1550Å doublet. The asymmetry of the line profiles in the STIS data reveals the presence of two absorbing components, not visible at the lower spectral resolution of *IUE*, where they are blended into a single gaussian.

Between *IUE* and *HST*, good quality high-resolution spectra have been obtained for about 25 hot DA white dwarfs, spanning a temperature range from 110 000 K down to 20 000 K. Using the latest heavy element blanketed non-LTE stellar atmosphere calculations, Barstow et al. (2003b) have addressed the heavy element abundance patterns. Completely objective measurements of abundance values and upper limits have been made using a χ^2 fitting technique to determine the uncertainties in the abundance measurements, which can be related to the formal upper limits in those stars where particular elements are not detected. This work shows that the presence or absence of heavy elements in the hot DA white dwarfs largely reflects what would be expected if radiative levitation is the supporting mechanism, although the measured abundances do not match the predicted values very well, as reported by other authors in the past. Almost all stars hotter than $\sim 50\,000\,K$ contain heavy elements.

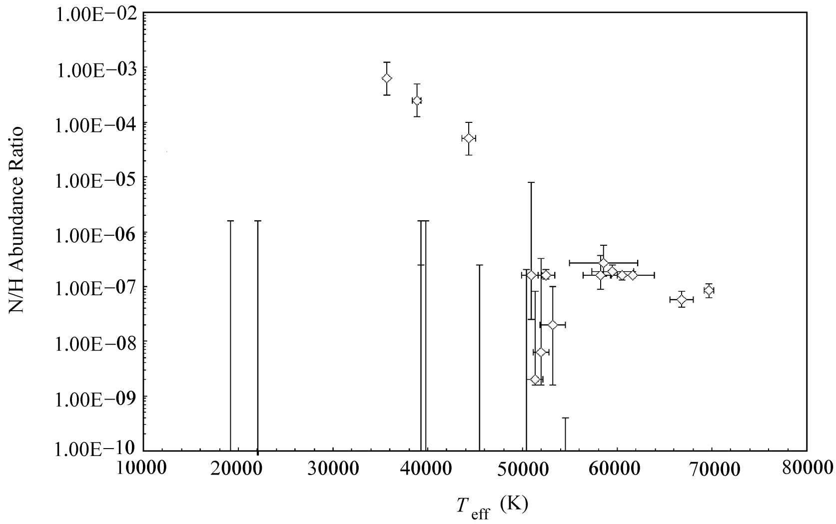

Fig. 13 Measured abundances of nitrogen (with respect to hydrogen) as a function of $T_{\rm eff}$ for a sample of 25 DA white dwarfs.

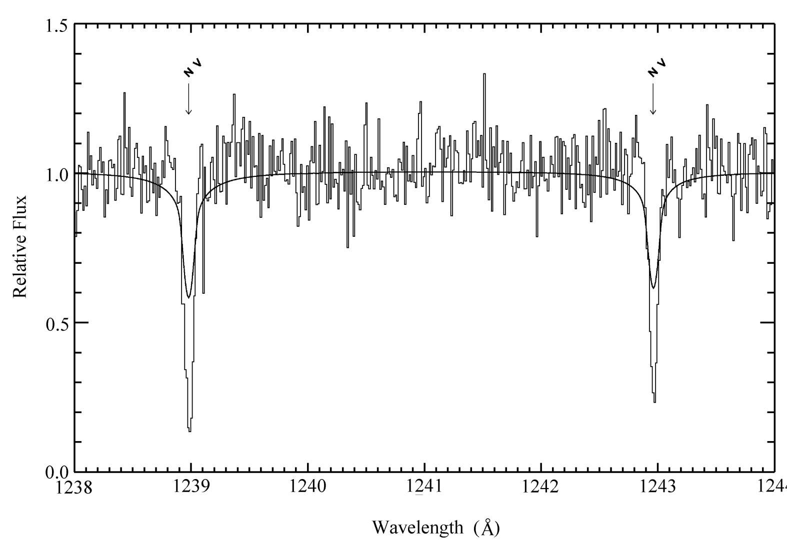

Fig. 14 STIS spectrum of REJ1032+532 in the region of the NV doublet (histogram), compared to the predicted line profiles from a homogeneous model atmosphere calculation.

For most stars the spread in element abundances is quite narrow and similar to the abundances measured in G191-B2B. However, there is an unexplained dichotomy at lower temperatures with some stars having apparently pure H envelopes and others detectable quantities of heavy elements. This is illustrated in Fig. 13, which shows the measured abundance of nitrogen as a function of $T_{\rm eff}$, a pattern that splits into two groups of stars at lower temperature. Three stars have high N abundances below ∼50 000K, while in the rest, only upper limits can be place on the N abundance. Furthermore, the observed spectra cannot be matched by models with a homogeneous composition but show that the material is located only in the outermost layers of the envelope. This is illustrated in Fig. 14, which shows the STIS spectrum of REJ1032+533 in the region of the NV doublet. The observed lines are very narrow and deeper than the profiles predicted by a homogeneous model calculation, which indicates that most of the nitrogen resides in the least dense, outer, layers of the atmosphere.

A few other strong temperature/evolutionary effects are seen in the UV abundance measurements. There is a decreasing Si abundance with temperature and a sharp decline in Fe and Ni abundance to zero, below ∼ 50 000 K. When detected, the Fe and Ni abundances maintain an approximately constant ratio, close to the cosmic value ∼ 20. For the hottest white dwarfs observed by STIS, the strongest determinant of abundance appears to be gravity. Qualitatively, these results are in keeping with physical models of diffusion and radiative levitation, but the detailed abundance measurements do not match predicted values.

5.3 EUV Spectroscopy

A great deal of detailed information has been obtained from analysis of UV spectra of DA white dwarfs and this observing technique will continue to be of tremendous importance. However, as some UV results already indicate, where the detailed line profiles suggest that photospheric material is not homogeneously mixed, they do not necessarily tell the whole story concerning the structure and composition of the photosphere. The emergent EUV flux from a hot white dwarf star is highly sensitive to both the effective temperature and composition of the envelope. Hence, EUV observations were recognized to have important diagnostic potential even before any EUV astronomy missions were actually flown. Barstow & Holberg (2003) have recently and extensively reviewed the development of EUV astronomy and some of the detailed results concerning white dwarfs. Therefore, this section discusses a subset of results that are particularly concerned with this review theme on the measurement of fundamental parameters of white dwarfs.

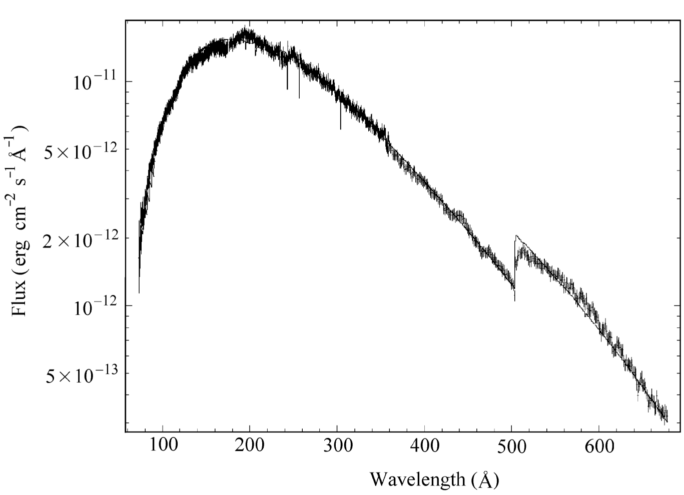

Fig. 15 EUV spectrum of the pure H atmosphere white dwarf HZ43, recorded with the *EUVE* spectrometers and described in the text.

Unlike the UV band, where high-resolution spectroscopy has been available for more than 20 years, the field of EUV astronomy has emerged more slowly, due to the greater difficulty of instrument development and practical observation in a region where the opacity of interstellar gas is at its greatest. Consequently, the spectrometers on board the *Extreme Ultraviolet Explorer* (*EUVE*) mission had relatively low effective area and modest spectral resolution ($R \sim 300$) compared to UV instrumentation. Nevertheless, since hot white dwarf fluxes peak in the EUV, detailed observations could be made of a significant sample of white dwarfs. Those white dwarfs with pure H envelopes are the most luminous at the shorter EUV wavelengths, as illustrated in Fig. 15, which shows an *EUVE* spectrum of the white dwarf HZ43. HZ43 was the first reported detection of an EUV source and has been studied frequently and, because of its pure H photosphere, often been used for calibration purposes. The flux corrected spectrum peaks near 200Å. The short wavelength decrease is determined entirely by the properties of the atmosphere but at long wavelengths, while some of the opacity is from the photosphere, the dominant effect is absorption by interstellar hydrogen and helium. Although interstellar opacity is not the topic of this review, a discussion of its characteristics in the EUV band is essential for understanding the photospheric results since photospheric He features could also be present at these same wavelengths in some stars. The interstellar features may interfere with or even completely mask any stellar component at the resolution of *EUVE*. The sharp step at 504Å is the HeI ISM absorption edge. The important HeII Lyman series lines also lie between the HeII edge at 228Å and the HeII Lyman α line at 304Å but the HeII column density is too low for a significant detection of these interstellar lines in HZ43. However, when the total interstellar HI column density is higher (a few $\times 10^{18}\,\mathrm{cm}^{-2}$ compared to $\sim 10^{18}\,\mathrm{cm}^{-2}$ for HZ43), and the HeI & HeII columns larger as a result, the HeII edge can be readily detected, along with the HeI autoionization edge at 206Å (Fig. 16).

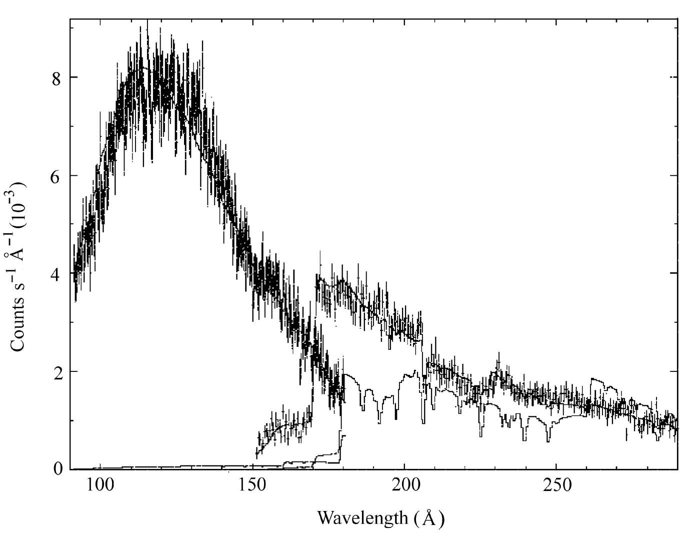

Fig. 16 *EUVE* count spectrum of the DA white dwarf GD659 (error bars), showing the HeI interstellar autoionization feature at 206Å and the interstellar HeII Lyman edge at 228Å. The solid histogram that matches the data is the best fit model spectrum for a pure H atmosphere, while the histogram that does not match the observed flux is a model including NV at an abundance inferred from the UV STIS spectrum assuming that the mixture is homogeneous.

If the white dwarf atmosphere contains significant quantities of elements heavier than H or He, the EUV spectrum is cut off very sharply at short wavelengths. Figure 17 shows the spectrum of the white dwarf G191–B2B, which is the proto-type "heavy element-rich" object. In this object the peak flux is at a wavelength ~ 260Å, with hardly any flux detectable below 200Å, in contrast to those stars with pure H envelopes. Initially, an understanding of the *EUVE* spectrum of G191–B2B and similar stars was quite elusive. First attempts to match the observation with synthetic spectra failed to reproduce either the flux level or even the general shape of the continuum (see Barstow et al. 1996 and Fig. 17). This problem was perceived to be due to the inclusion of an insufficient number of Fe and Ni lines. Adding some 9 million predicted lines to the few thousand with measured wavelengths did provide a self-consistent model able to reproduce the EUV, UV and optical spectra (Lanz et al. 1996). However, good agreement between the observed *EUVE* spectrum and the model prediction could only be achieved by inclusion of a significant quantity of helium, either in the stellar photosphere or as an ionised interstellar/circumstellar component. Unfortunately, due to the limited resolution of *EUVE* (~ 0.5Å) in the region of the HeII Lyman series, this inferred He contribution could not be directly detected.

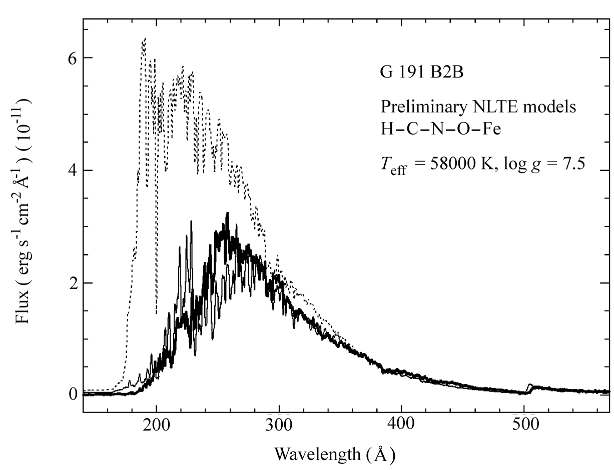

Fig. 17 *EUVE* spectrum of G191–B2B (thick solid line) compared with two non-LTE line-blanketed models for $T_{\rm eff}$=58 000 K, $\log g = 7.5$. The dashed model includes blanketing from 6000 lines of Fe and Ni, while the thin solid line includes 300 000 lines.

The nature of the He opacity, if really present, is problematic. If all of it is interstellar, the implied He ionization fraction is much larger (by a factor ~ 2) than the 30%–40% typical of the nearby ISM. Furthermore, the level of agreement between model and data at short wavelengths, below ~ 200Å, is poor, the predicted flux exceeding that observed by a factor ~ 10 (Fig. 18). Empirically, Barstow et al. (1999) showed that the overall flux distribution could be matched by assuming a different Fe abundance for models separately applied to the short (< 190Å) and long (> 190Å) ranges. Examination of the formation depths of the Fe lines at different wavelength hints at an explanation of the problem (Fig. 19), showing that the formation depth has a strong wavelength dependence and indicating that abundance measurements made in the UV and EUV, and even in different parts of the EUV, are sampling quite different regions of the atmosphere. Therefore, the results imply that the Fe is not distributed homogeneously in the atmosphere, but has different abundances at different depths. A fairly simple model, dividing the atmosphere into two "slabs" with a lower Fe abundance in the outer region (Fe/H=10^{-6} cf. 4×10^{-5}) provides a good, but not completely unique, match to the data (Fig. 20). Subsequently,

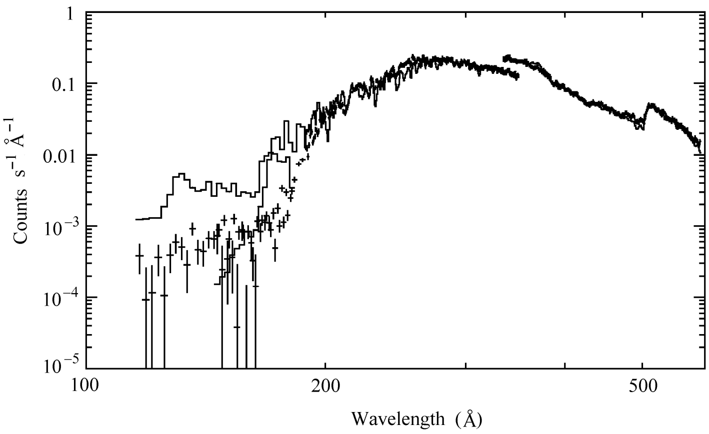

Fig. 18 Comparison of the complete *EUVE* spectrum of G191–B2B (error bars) with a single model that give the optimum match to the > 180Å wavelength range. Discontinuities near 170 and 320Å are regions where the *EUVE* spectrometer channels overlap, and arise from differing spectrometer effective area. The predicted short wavelength flux is a factor 5–10 greater than that observed.

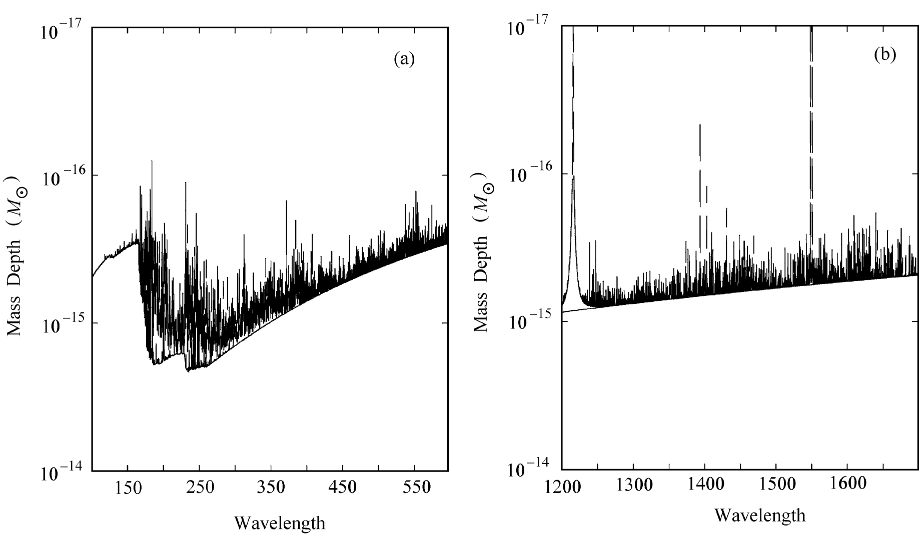

Fig. 19 Mass depth (total mass above the point of interest) of the line (upper, dashed curve) and continuum (lower curve) formation at monochromatic optical depth $\tau_\upsilon = 2/3$ as a function of wavelength in the EUV and far UV.

important progress has been made in incorporating radiative levitation and diffusion self-consistently into the atmosphere calculations to give predictions of the depth dependent abundance profiles a firm physical basis (Dreizler & Wolff 1999; Schuh et al. 2001, 2002). Interestingly, the Fe profile determined from these calculations is similar to the simple slab model of Barstow et al. (1999), but with a smoother transition region between the two main regions.

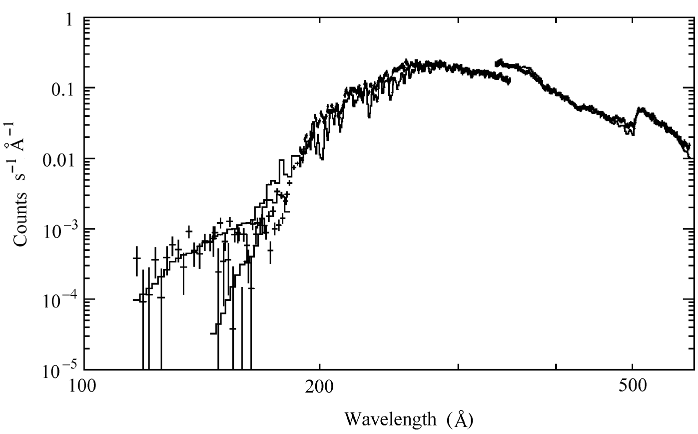

Fig. 20 Comparison of the complete *EUVE* count spectrum of G191-B2B with the "slab" model of Fe depth dependent abundance described in the text.

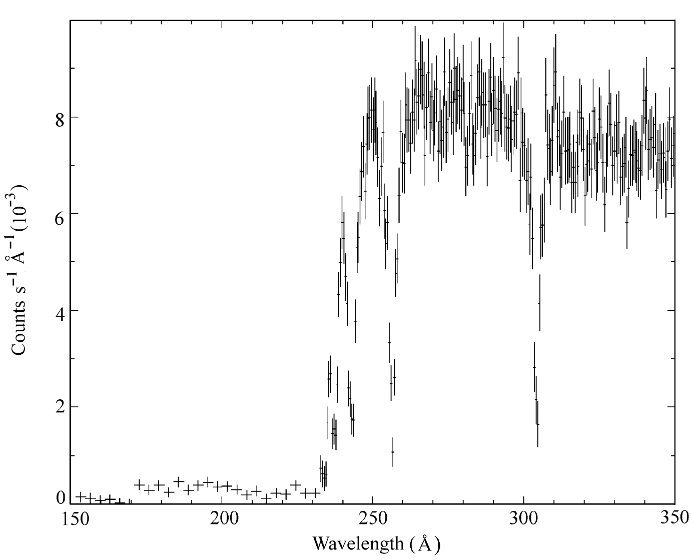

Fig. 21 *EUVE* spectrum of the massive DA white dwarf GD50, showing the presence of photospheric HeII.

The need for a He opacity component, required to provide a good match to the homogeneous models, is reduced in the stratified models but not eliminated. Although, in principle EUV observations are more sensitive to the presence of He than any other waveband, there have been few real detections of the element in *EUVE* spectra. One example is the massive DA star GD50, where the HeII Lyman line series is clearly visible (Fig. 21). However, because of the high mass ($1.2\,M_\odot$), it is likely that the star is a product of binary evolution and other stars where He has been detected are in known binary systems. Therefore, the issue of whether or not photospheric He is present in the hottest DA white dwarfs still needs to be resolved.

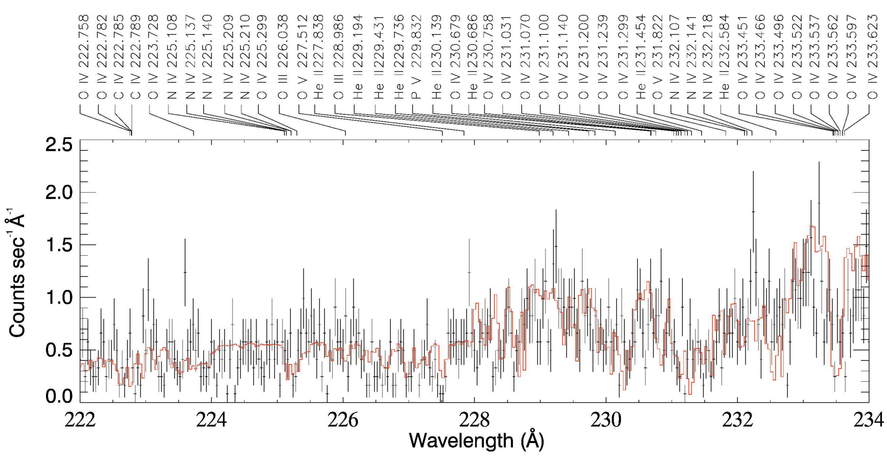

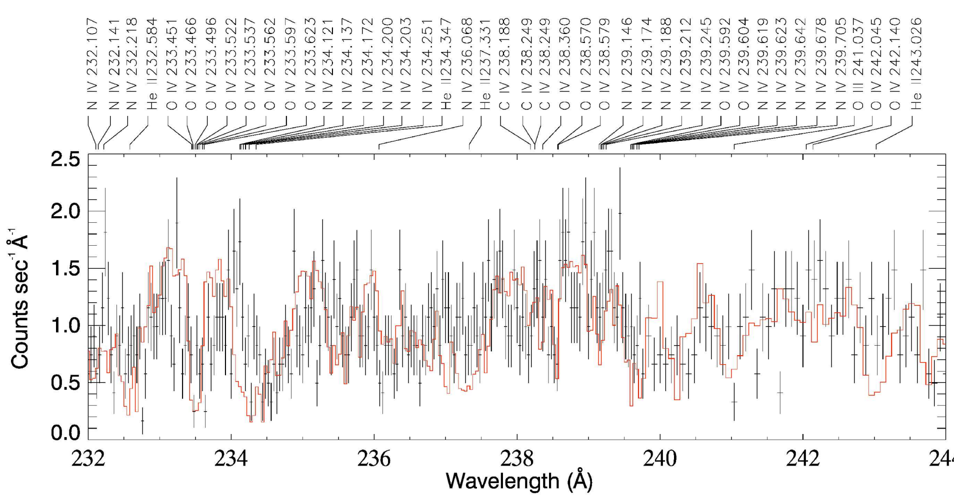

Fig. 22 High-resolution EUV spectrum of G191–B2B, obtained with the J-PEX spectrometer, spanning the wavelength range 222–244 Å (error bars). The red histogram is the best-fit theoretical model of the star and ISM, as described in the text. The strongest predicted lines of He, C, N, O, and P are labeled with their ionization state and wavelength. Lines of Fe and Ni are too numerous to include here and account for the unlabelled individual features and broader absorption structures.

Direct detection of He in those stars with significant heavy element opacity requires higher spectral resolution than was achieved with *EUVE*, to separate the HeII Lyman lines from the much larger number from other elements. Recent developments in normal incidence optics have allowed the construction of a new generation of spectrographs combining high throughput with high spectral resolution. Thus far, the technique has only been applied on short duration sounding rocket flights, with exposure times far shorter than available with satellite missions. The spectrum of G191-B2B, obtained with the *J-PEX* mission, shows the promise of future instrumentation and partially solves the problem of the He inferred from the *EUVE* analyses (Fig. 22, Cruddace et al. 2002). He is certainly directly detected and the best-fit model requires both interstellar and photospheric components. However, only the interstellar complex in the 228–230Å range is detected directly. The predicted strength of the photospheric HeII line at 243Å is at a level similar to the signal-to-noise in that part of the spectrum and so a significant detection of photospheric He cannot be claimed at this stage. Further analysis of the spectrum indicates that the interstellar HeII has two components, one associated with the local ISM and a second that may be related to the circumstellar material detected in the far-UV (Barstow et al. 2003c).

6 CONCLUSION

This paper has reviewed the range of techniques applied to measuring the parameters of the hot, hydrogen-rich white dwarf stars. The principal direct measurements are of effective temperature, surface gravity and photospheric composition. From these it is possible to infer more fundamental information such as the stellar mass and radius, which are essential for the calculation of cooling rates and the use of the white dwarf population to study the history and evolution of the galaxy. Spectroscopic data from a variety of wavelength ranges are required for this work and the important contributions from optical, ultraviolet and extreme ultraviolet studies have been outlined. While some important results have been obtained, a number of important questions remain to be answered. Continued access to high-resolution spectroscopy in the far-UV and a new, similar capability in the EUV will be essential to provide final solutions for the outstanding problems.

Apart from a very few white dwarfs, where dynamically determined masses are available, we rely on the theoretical white dwarf mass-radius relation to determine these parameters from the values of $T_{\rm eff}$ and $\log g$. The issue of the accuracy of the theoretical mass-radius calculations is an important one and the discovery of a sample of white dwarfs in binary systems, from which we might ultimately extend the number of objects for which we have dynamical masses, indicates that we might finally be able to make a definitive test of this Nobel Prize-winning theory.

Acknowledgements MAB is grateful to the many collaborators with whom he has worked in this field for the last ~ 20 years. He acknowledges the support of the Particle Physic and Astronomy Research Council, UK.

References

Bannister N. P., Barstow M. A., Holberg J. B., Bruhweiler F. C., 2001, In: J. L. Provencal, H. L. Shipman, J. MacDonald, S. Goodchild, eds., ASP Conf. Ser. Vol. 226, 12th European Workshop on

White Dwarfs, San Francisco: ASP, p.105
Barstow M. A., Bond H. E., Burleigh M. R., Holberg J. B., 2001a, MNRAS, 322, 891
Barstow M. A., et al., 1993, MNRAS, 264, 16
Barstow M. A., Good S. A., Burleigh M. R., Hubeny I., Holberg J. B., Levan A. J., 2003a, MNRAS, in press
Barstow M. A., Good S. A., Holberg J. B., Hubeny I., Bannister N. P., Bruhweiler F. C., Burleigh M. R., Napiwotzki R., 2003b, MNRAS, 341, 870
Barstow M. A. et al., 2003, Proc SPIE, 4854, 654
Barstow M. A., Holberg J. B., Extreme Ultraviolet Astronomy, Cambridge University Press
Barstow M. A., Holberg J. B., Cruise A. M., Penny A. J., 1997, MNRAS, 286, 58
Barstow M. A., Holberg J. B., Fleming T. A., Marsh M. C., Koester D., Wonnacott D., 1994, MNRAS, 270, 499
Barstow M. A., Holberg J. B., Hubeny I., Good S. A., Levan A. J., Meru F., 2001b, MNRAS, 325, 211
Barstow M. A., Hubeny I., Holberg J. B., 1998, MNRAS, 299, 520
Barstow M. A., Hubeny I., Holberg J. B., 1999, MNRAS, 307, 884
Barstow M. A., Hubeny I., Lanz T., Holberg J. B., Sion E. M., 1996, In: S. Bowyer, R. F. Malina, eds., Astrophysics in the Extreme Ultraviolet, Dordrecht: Kluwer, p.203
Bergeron P., Saffer R., Liebert J., 1992, ApJ, 394, 228
Blöcker T., 1995, A&A, 297, 727
Blöcker T., Herwig F., Dreibe T., Bramkamp H., Schönberner D., 1997, In: J. Isern, M. Hernanz, E. Garcia-Berro, eds, White Dwarfs, Dordrecht: Kluwer, p.57
Bruhweiler F. C., Kondo Y., 1983, ApJ, 269, 657
Burleigh M. R., Barstow M. A., Fleming T. A., 1997, MNRAS, 287, 381
Chandrasekhar S., 1931, ApJ, 84, 81
Chandrasekhar S., 1935, MNRAS, 95, 226
Chayer P., Fontaine G., Wesemael F., 1995, ApJS, 99, 189
Cruddace R. G. et al., 2001, ApJ, 565, L47
Dreizler S., Wolff B., 1999, A&A, 348, 189
Dupree A. K., Raymond J. C., 1982, ApJ, 263, L63
Fowler R. H., 1926, MNRAS, 87, 114
Hamada T., Salpeter E. E., 1961, ApJ, 134, 683
Holberg J. B., Barstow M. A., Sion E. M., 1998, ApJS, 119, 207
Holberg J. B. et al., 1993, ApJ, 416, 806
Holberg J. B., Hubeny I., Barstow M. A., Lanz T., Sion E. M., Tweedy R. W., 1994, ApJ, 425, L205
Marsh M. C. et al., 1997, MNRAS, 286, 369
Mestel L., 1952, MNRAS, 112, 583
Napiwotzki R., Green P. J., Saffer R. A., 1999, ApJ, 517, 399
Oppenheimer B. et al., 2001, Science, 282, 698
Schatzmann E., 1958, White Dwarfs, Amsterdam: North Holland Publishing Co.
Schuh S., Drezler S., Wolff B., 2001, In: J. L. Provencal, H. L. Shipman, J. MacDonald, S. Goodchild, eds., ASP Conf. Ser. Vol. 226, 12th European Workshop on White Dwarfs, San Francisco: ASP, p.79
Schuh S., Dreizler S., Wolff B., 2002, A&A, 382, 164
Vennes S., Bowyer S., Dupuis J., 1996, ApJ, 461, L103
Vennes S., Christian D., Thorstensen J. R., 1998, ApJ, 502, 763
Vennes S., Pelletier C., Fontaine G., Wesemael F., 1988, ApJ, 331, 867
Wood M. A., 1992, ApJ, 386, 539
Wood M. A., 1995, In: D. Koester, K. Werner, eds., Lecture Notes in Physics, White Dwarfs, Berlin: Springer, p.41